Narrow-Gap Luttinger Liquid in Carbon Nanotubes

L. S. Levitov[1] and A. M. Tsvelik[2]

[1]*Department of Physics, Center for Material Sciences & Engineering, Massachusetts Institute of Technology, 77 Massachusetts Avenue, Cambridge, Massachusetts 02139*

[2]*Department of Physics, Brookhaven National Laboratory, Upton, New York 11973-5000*

(Received 16 May 2002; published 2 January 2003)

Electron interactions reinforce minigaps induced in metallic nanotubes by an external field and turn the gap field dependence into a universal power law. An exactly solvable Gross-Neveau model with an SU(4) symmetry is derived for neutral excitations near half filling. Charge excitations, described by a sine-Gordon perturbation of Luttinger liquid theory, are composite solitons formed by the charged and neutral fields with two separate length scales. Charge compressibility at finite density, evaluated in terms of intersoliton interaction, exhibits a crossover from overlapping to nonoverlapping soliton state. Implications for the Coulomb blockade measurements are discussed.

DOI: 10.1103/PhysRevLett.90.016401 PACS numbers: 71.10.Pm, 72.80.Sk

Electron interactions create a peculiar strongly correlated 1D electron system [1–5] in single-wall metallic Cabon nanotubes, the thinnest and the cleanest among the currently available nanoscale quantum wires. Luttinger liquid theory of nanotubes predicts [1,2] that, since tube diameter is larger than carbon separation, the 1D electron coupling is mainly accounted for by the long-range electron interaction (forward scattering), while the exchange and umklapp scattering, as well as backscattering, are relatively weak [5]. Recent experimental work [6–8] focused on Luttinger liquid effects in tunneling, observed as characteristic power laws in the tunneling current dependence on bias voltage and temperature.

Here we discuss Luttinger liquid effects in single-wall nanotubes with a minigap at the band center induced by an external perturbation. Such a minigap can be opened by parallel magnetic field [9] or by the intrinsic curvature of the tube [10]. The field- and curvature-induced gaps were observed experimentally [11,12] and found to be in agreement with the noninteracting electron model. We show that electron interaction enhances the charging gap and makes it a power law function of the bare gap.

This provides a unique situation, not available in other quantum wires, when Luttinger liquid effects are manifest in thermodynamical properties. For instance, in a gapped state induced by magnetic field, the bare gap is determined without any fitting parameters by Aharonov-Bohm flux through tube cross section, while the charging gap is directly measurable via Coulomb blockade, a prominent feature of transport in nanotubes [13–18]. In the strong forward scattering limit, the power law relation of the charging gap and magnetic field is characterized by a universal exponent 4/5. We emphasize that the charging gap measurement is qualitatively different from the tunneling current measurement because it can be performed in thermodynamic equilibrium.

Also, in the presence of interactions the charging gap is much enhanced compared to the neutral excitation gap, while in a noninteracting system the two gaps are precisely equal. Large energy separation of the charged and neutral sectors results in high symmetry of the states in the neutral sector described by multiplets of the group $O(6) \sim SU(4)$ derived from the exactly solvable Gross-Neveau model. This picture, demonstrated in the situation when the gapped state is created by external field, is realistic, since the intrinsic interaction-induced gap in nanotubes is believed to be extremely small.

Electron bands of metallic single-wall tubes form two pairs of spin-degenerate right and left branches intersecting at the band center [19]. The Hamiltonian in the forward scattering approximation [1,2] has the form

$$\mathcal{H}_0 = -i\hbar v \int \sum_{j=1}^{4} \psi_j^+ \sigma_3 \partial_x \psi_j dx + \frac{1}{2}\sum_q \rho_q V(q) \rho_{-q}, \tag{1}$$

where $\psi_j(x)$ is a two component wave function, $\rho(x) = \sum_{j=1}^{4} \psi_j^+(x)\psi_j(x)$ is charge density, and v is Fermi velocity. The form of the forward scattering amplitude in Eq. (1) depends on the electrostatic environment. In a nanotube of radius r, in the absence of screening, $V(q) = \int V(x) e^{iqx} dx = e^2 \ln[(qr)^{-2} + 1]$. The substrate dielectric constant ϵ reduces $V(q)$ by a factor $2/(\epsilon + 1)$.

A field-induced gapped state [9,10] is described by adding to the Hamiltonian (1) a backscattering term

$$\mathcal{V}_{\text{ext}} = \Delta_0 \int \sum_{j=1}^{4} \psi_j^+ \sigma_1 \psi_j dx. \tag{2}$$

In the absence of interactions, $V(q) = 0$, the electron spectrum is $\epsilon(p) = \pm(v^2 p^2 + \Delta_0^2)^{1/2}$ with the value of Δ_0 depending on the backscattering mechanism. The magnetic field-induced gap [9] is linear in the field: $\Delta_0 = \hbar v \phi / r$, where $\phi = \pi r^2 B/\Phi_0$ is the flux through the tube cross section scaled by $\Phi_0 = hc/e$. For the typical tube radius $r \simeq 0.5$ nm and $B \simeq 10$ Tesla, the gap $\Delta_0 \simeq 10$ meV.

We bosonize the Hamiltonian $\mathcal{H} = \mathcal{H}_0 + \mathcal{V}_{\rm ext}$ in the standard way, using $\psi_j \propto r^{-1/2}\exp(i\sqrt{\pi}\Phi_j)$. The Gaussian part $\mathcal{H}_0$ is diagonalized using linear combinations of the bosonic fields $\Phi_j = (e_j^a\phi_a)$ with $\mathbf{e}_0 = \frac{1}{2}(1,1,1,1)$ and the unit vectors $\mathbf{e}_{1,2,3}$ orthogonal to $\mathbf{e}_0$ and each other. In this basis the Gaussian part of the Lagrangian describes one charged and three (neutral) flavor modes:

$$\mathcal{L}_0 = \frac{1}{2}\sum_q \{\partial_\tau\phi_0(q)\partial_\tau\phi_0(-q) + K_q q^2\phi_0(q)\phi_0(-q)\} + \frac{1}{2}\int dx \sum_{a=1}^{3}(\partial_\mu\phi_a)^2, \quad K_q = 1 + \frac{4}{\pi}V(q) \tag{3}$$

($\hbar = v = 1$). Bosonizing $\mathcal{V}_{\rm ext} = \Delta_0\int dx\sum_{j=1}^4(R_j^+L_j + \text{H.c.})$, we have

$$\mathcal{L}_\lambda = -2\lambda\int dx\left(\sum_{j=1}^{4}\cos\sqrt{4\pi}\Phi_i\right) \tag{4}$$

with $\lambda = \Delta_0/r$. The total Lagrangian $\mathcal{L} = \mathcal{L}_0 + \mathcal{L}_\lambda$ displays the fundamental U(1) × SU(4) symmetry playing a major role in our analysis. Forward scattering makes the perturbation (4) even more relevant. At zero chemical potential the coupling λ grows under renormalization and opens spectral gaps.

There are several possible regimes in which a nanotube, described by Eqs. (3) and (4), may exist. First, there is an insulating regime with the density at half filling, where all excitations are gapped. Second, there are conducting states which can be realized by applying various external fields. These fields may close some gaps or even all of them, provided their magnitudes exceed certain critical values. For example, by varying chemical potential one can close all the gaps and make the perturbation λ irrelevant. This will lead to a transition into a metallic (Tomonaga-Luttinger liquid) regime. Fields breaking the SU(4) symmetry will not affect the charge sector and thus leave the system insulating, but may close some of the gaps in the flavor sector.

From Lagrangian (3) we obtain the scaling dimension of the operator $(R_j^+L_j + \text{H.c.})$, equal to $d = (3+\alpha)/4$ with $\alpha = K^{-1/2}$. The renormalization group (RG) establishes the following general relationship between the bare coupling constant and the spectral gap: $\Delta/D \sim \lambda^{1/(2-d)}$. Since the velocity in the charge sector undergoes a strong increase, we also conclude that the charge gap contains an additional numerical factor such that the charge and flavor gaps are related to the noninteracting gap Δ_0 as

$$\Delta_{\rm fl} \simeq \Delta_0(D/\Delta_0)^{(1-\alpha)/(5-\alpha)}, \qquad \Delta_{\rm ch} \simeq K^{1/2}\Delta_{\rm fl}, \tag{5}$$

where $D = \hbar v/r$ is 1D bandwidth. Since Δ_0 is proportional to the external magnetic field, Eq. (5) predicts a power law scaling of the gaps versus an experimentally controllable parameter. For high charge stiffness $K_q \gg 1$, the gap scaling exponent is universal, with the value 4/5.

The separation (5) of energy scales, originating from the sharp difference in the velocities in the charge and flavor sectors, enables one to integrate out the fast mode ϕ_0 in the adiabatic approximation. This will generate an effective action for the flavor modes with SU(4) symmetry. Separating ϕ_0 in the Lagrangian (4) one obtains

$$\mathcal{L}_\lambda = -4\lambda\int dx(u_1\cos\tilde{\boldsymbol{\phi}}_0 + u_2\sin\tilde{\boldsymbol{\phi}}_0), \tag{6}$$

$$u_1 = \prod_{a=1}^{3}\cos\tilde{\boldsymbol{\phi}}_a, \qquad u_2 = \prod_{a=1}^{3}\sin\tilde{\boldsymbol{\phi}}_a, \tag{7}$$

where $\tilde{\boldsymbol{\phi}}_i = \sqrt{\pi}\boldsymbol{\phi}_i$. Treating the slow fields u_i as adiabatic parameters and shifting the variable

$$\phi_0 \to \phi_0 + \eta, \qquad \eta = \pi^{-1/2}\tan^{-1}(u_2/u_1), \tag{8}$$

we transform the total Lagrangian $\mathcal{L} = \mathcal{L}_0 + \mathcal{L}_\lambda$ as

$$\mathcal{L} = \mathcal{L}_0[\phi_0 + \eta] - \int dx M[\phi_a]\cos\tilde{\boldsymbol{\phi}}_0 \tag{9}$$

with $M[\phi_a] = 2\lambda(1 + \sum_{a\neq b}\cos2\tilde{\boldsymbol{\phi}}_a\cos2\tilde{\boldsymbol{\phi}}_b)^{1/2}$. From Eq. (9) we derive an effective action for the flavor sector valid for energies well below the charge gap (5) by integrating over the fast mode ϕ_0. Let us examine the results of this integration. Writing the first term in (9) as $\mathcal{L}_0[\phi_0] + \mathcal{L}_0[\eta] + \sum_{\omega,q}\{\phi_0\}_q(\omega^2 + K_q q^2)\{\eta\}_q$ we note that the η-dependent terms are strongly irrelevant. For example, $\mathcal{L}_0[\eta]$ contains squares of the gradients

$$\partial_\mu\eta = \frac{\partial_\mu\phi_1\sin2\tilde{\boldsymbol{\phi}}_2\sin2\tilde{\boldsymbol{\phi}}_3 + \text{permut.}}{1 + \sum_{a\neq b}\cos2\tilde{\boldsymbol{\phi}}_a\cos2\tilde{\boldsymbol{\phi}}_b} \tag{10}$$

consisting of a series of operators with the minimal scaling dimension 2. The relevant contribution arises from the last term of Eq. (9). Integrating it over ϕ_0 we obtain the ground state energy of the sine-Gordon model

$$-M^{2/(2-\alpha/4)}[\phi_a] = -g\sum_{a\neq b}:\cos2\tilde{\boldsymbol{\phi}}_a\cos2\tilde{\boldsymbol{\phi}}_b: + \ldots, \tag{11}$$

where g is a suitably renormalized coupling constant and dots stand for less relevant operators. The normal ordering is taken with respect to the new cutoff G.

Thus at energies smaller than the cutoff G we obtain the effective action for the flavor modes in the form of the O(6) ~ SU(4) Gross-Neveau model:

$$\mathcal{L} = \int dx\left[\frac{1}{2}\sum_{a=1}^{3}(\partial_\mu\phi_a)^2 - g\sum_{a\neq b}:\cos2\tilde{\boldsymbol{\phi}}_a\cos2\tilde{\boldsymbol{\phi}}_b:\right] = \int dx[i\bar{\chi}_j\gamma_\mu\partial_\mu\chi_j - g:(\bar{\chi}_j\chi_j)(\bar{\chi}_k\chi_k):], \tag{12}$$

where χ_j ($j = 1, ..., 6$) are Majorana fermions. We emphasise that the SU(4) symmetry here is exact being a symmetry of the original Hamiltonian. This makes this model quite distinct from the effective models suggested in [20,21], where high symmetries are supposed to emerge at low energies as a result of renormalization.

The model (12) is exactly solvable [22]; the spectrum consists of $3+6+3$ relativistic particles with masses $m, \sqrt{2}m, m$ transforming according to different representations of the O(6) $\sim$ SU(4) group. Their dispersion law is $E_i(p) = (v^2p^2 + m_i^2)^{1/2}$. The Majorana fermions themselves belong to the vector representation of the group and carry mass $\sqrt{2}m$. The mass m coincides with the spin gap $\Delta_{\rm fl}$ estimated by the RG equation (5), while the coupling constant g in the Gross-Neveau model (12) is fixed by the requirement that the latter model yields the correct neutral excitation spectrum at the energies well below the charge gap $\Delta_{\rm ch}$.

The charge sector, described by the field ϕ_0, contains nontopological neutral exciton modes as well as charged topological excitations (solitons and antisolitons). To obtain the spectrum of exciton modes, we linearize the Lagrangian (9) in ϕ_0 near the saddle point $\phi_i = 0$ (the cosine maximum), which gives $\omega^2 = K(q)v^2q^2 + 4\pi M$ with $M \simeq \Delta_{\rm fl}^2$. Thus the exciton spectral gap is of the same order as the flavor gap.

As for the topological charge excitations, they carry exactly the same quantum numbers as an electron. This happens because whenever a soliton of ϕ_0 is created, it acts as an effective potential in the presence of which the flavor fields form bound states. The flavor fields coupled to a ϕ_0 soliton give it the corresponding quantum numbers. To elaborate on this we consider the process of soliton formation in more detail.

In the original sine-Gordon problem (3) and (4), an electron is represented by a soliton of one of the fields Φ_j. Soliton spatial size can be estimated from a variational principle. Because of large charged stiffness K, the elastic energy of the soliton is dominated by the field ϕ_0. According to (3) and (4), the soliton energy, estimated from the energy in the space interval l, where the field $\Phi_j(x)$ varies, is $E(l) \simeq (K_{ql=1}l^{-2} + \lambda')l$ with renormalized coupling $\lambda'(l) = \lambda(r/l)^{(3+\alpha)/4}$. Soliton size w can be found by minimizing the energy with respect to l. Ignoring the logarithmic l dependence of K, this gives $w \approx [K/\lambda'(w)]^{1/2}$. The soliton energy $E(w) \simeq [K\lambda'(w)]^{1/2}$ coincides with the charge gap $\Delta_{\rm ch}$ in (5).

A peculiar feature of the composite charge soliton is the presence of two different length scales, because the flavor fields $\phi_{1,2,3}$ vary faster than the stiffer charge field ϕ_0. Let us consider a variational solution of the problem $\mathcal{L}_0 + \mathcal{L}_\lambda$ with one of the fields Φ_j varying between two minima of the energy (4). To be specific, we consider a soliton of the field $\Phi_1 = \frac{1}{2}(\phi_0 + \cdots + \phi_3)$ in which Φ_1 changes by $\sqrt{\pi}$, while $\Phi_{1,2,3}$ do not change. In this case all fields $\tilde\phi_{0,\ldots,3}$ change by $\pi/2$. The length w over which the field ϕ_0 changes is much larger than that for $\phi_{1,2,3}$. Thus the variational problem for $\tilde\phi_0$ can be treated in a $\pi/2$ step approximation for $\tilde\phi_{1,2,3}$, as

$$\tfrac{1}{2}K(\tilde\phi_0')^2 = 4\pi\lambda'[1 - \max(\cos\tilde\phi_0, \sin\tilde\phi_0)] \qquad (13)$$

(we treat K as a constant). The solution of Eq. (13) with $\tilde\phi_0 = \pi/4$ at $x = 0$, and the cos and sin terms contributing separately in the regions $x > 0$, $x < 0$, is

$$\tilde\phi_0(x) = \begin{cases} 2\cos^{-1}\tanh(u - x/w), & x < 0, \\ \frac{\pi}{2} - 2\cos^{-1}\tanh(u + x/w), & x > 0, \end{cases} \qquad (14)$$

where $w = (K/4\pi\lambda')^{1/2} = \hbar v/\Delta_{\rm ch}$, $u = \tanh^{-1}(\cos\pi/8)$.

The problem for the flavor fields is simplified because they vary in the region where $\tilde\phi_0 \approx \pi/4$. This gives

$$\tfrac{3}{2}\tilde\phi'^2 = 2^{3/2}\pi\lambda'(1 - \cos^3\tilde\phi - \sin^3\tilde\phi), \qquad (15)$$

where $\tilde\phi = \tilde\phi_{1,2,3}$. Integrating Eq. (15) we obtain the function $\tilde\phi(x)$. As illustrated in the Fig. 1 inset, the $\tilde\phi_0$ step is $\sim\sqrt{K}$ times wider than the $\tilde\phi_{1,2,3}$ step. We emphasize that composite solitons in which all four fields $\tilde\phi_i$ vary are charge excitations of the lowest possible energy.

Now we consider multisoliton solutions and determine charge compressibility from intersoliton interaction. The compressibility $\chi \equiv (d^2E_n/d^2n)^{-1}$, with n the electron density, is directly related to the capacitance $C = dn/dV_g$ and the charging spectrum measured in a Coulomb blockade experiment. The charging spectrum peak spacing is $\delta_n = E_{n+1} - 2E_n + E_{n-1} \approx \chi^{-1}$. We consider densitites smaller than l_s^{-1} for which the charge fields ϕ_0 of different solitons may overlap, while the neutral cores with steps of $\phi_{1,2,3}$ are isolated. The effective energy of the field ϕ_0 is obtained by minimizing (6) with respect to $\tilde\phi_{1,2,3}$ at each value of $\tilde\phi_0$, which gives $-4\lambda' \max_m \cos(\tilde\phi_0 + \frac{\pi}{2}m)$. Switching between different branches occurs at $\tilde\phi_0 = \frac{\pi}{4} + \frac{\pi}{2}m$. Approximating cos by a parabola near each maximum one obtains

$$U(\tilde\phi_0) = 2\lambda' \min_m(\tilde\phi_0 - \pi m/2)^2. \qquad (16)$$

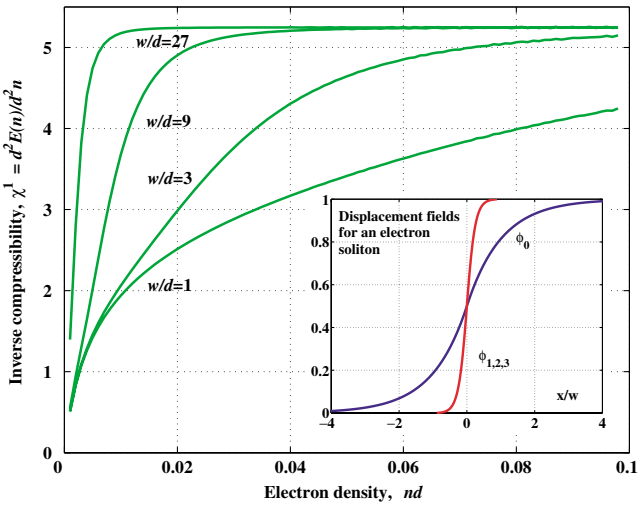

FIG. 1 (color online). Inverse charge compressibility scaled by $\hbar v$ plotted for several soliton widths $w = (4\pi\lambda')^{-1/2}$. Equation (23) was used with the screening length $l_s = 0.2\ \mu$m, $v = 8 \cdot 10^7$ cm/s, $\epsilon = 12$, tube diameter $d \equiv 2r = 1$ nm. Inset: electron soliton charge and flavor parts [Eqs. (14) and (15)] scaled by $\pi/2$, with the stiffness $K = 16$. Step widths for $\tilde\phi_0$ and $\tilde\phi_{1,2,3}$ differ by $K^{1/2}$.

This approximation is extremely accurate, as one can check by comparing Eq. (14) with the soliton solution

$$\tilde{\phi}_0(x) = \begin{cases} \frac{\pi}{4} e^{x/w}, & x < 0, \\ \frac{\pi}{2} - \frac{\pi}{4} e^{-x/w}, & x > 0 \end{cases} \tag{17}$$

of the variational problem for the total energy

$$E[\tilde{\phi}_0] = \int dx \left(\frac{1}{2\pi} \partial_x \tilde{\phi}_0 \hat{K} \partial_x \tilde{\phi}_0 + U(\tilde{\phi}_0) \right) \tag{18}$$

with the interaction kernel $\hat{K} = \delta(x - x') + \frac{4}{\pi} V(x - x')$.

In a soliton lattice the field $\tilde{\phi}_0(x)$ is a continuous monotonic function with smooth $\pi/2$ steps, as in the Fig. 1 inset. To evaluate the energy (18), we introduce a periodic *discontinuous* field $\varphi = \tilde{\phi}_0 - \pi m/2$ with integer m chosen to minimize $U(\tilde{\phi}_0)$. The energy (18) with $\tilde{\phi}_0 = \varphi - \frac{\pi}{2} \sum_m \theta(x - ma)$ takes the form

$$\int dx \left\{ \frac{1}{2\pi} \left[\partial_x \varphi + \frac{\pi}{2} G(x) \right] \hat{K} \left[\partial_x \varphi + \frac{\pi}{2} G(x) \right] + 2\lambda' \varphi^2 \right\}, \tag{19}$$

where $G(x) = \sum_m \delta(x - ma)$. The advantage of the form (19) is that this *quadratic* function can be easily minimized in the Fourier representation. We obtain

$$\varphi(q) = -iq \frac{\pi}{2} G(q) K_q / (K_q q^2 + 4\pi\lambda') \tag{20}$$

with $G(q) = 2\pi \sum_n \delta(qa - 2\pi n)$. The energy of (20) is

$$E[\varphi] = \sum_q 4\lambda' K_q \left(\frac{\pi}{2} G(q) \right)^2 \Big/ (K_q q^2 + 4\pi\lambda'). \tag{21}$$

Using the identity $G^2(q) = LG(q)$, with L the system size, the energy density can be written as

$$E(n) = \hbar v \frac{\pi n^2}{8} \sum_{m=-\infty}^{\infty} \frac{4\pi\lambda' K_{q_m}}{K_{q_m} q_m^2 + 4\pi\lambda'} \tag{22}$$

with $q_m = 2\pi m/a$ and soliton density $n = 1/a$.

Charge compressibility $\chi = [d^2E(n)/d^2n]^{-1}$ obtained from Eq. (22) with

$$K(q) = 1 + \frac{2}{\epsilon + 1} \frac{4e^2}{\pi\hbar v} \ln[(q^2 + r^{-2})/(q^2 + l_s^{-2})] \tag{23}$$

that models screening (e.g., by a gate) at distance $l_s \gg r$ is plotted in Fig. 1. At high density $n \gg w^{-1}$, compressibility is density independent, $\chi_0^{-1} = \frac{\pi}{4} \hbar v + \frac{4e^2}{\epsilon+1} \ln(l_s/r)$. At lower $n \ll w^{-1}$ it varies as $\chi^{-1} = \chi_0^{-1} - \frac{4e^2}{\epsilon+1} \ln(rn)$. The overlapping solitons ($nw > 1$) interact via $V(r) \propto r$, while nonoverlapping solitons interaction (at $nw < 1$) is $V(r) \propto 1/r$, because electric field is screened and confined to 1D at $r \leq w$ and becomes deconfined at $r \geq w$.

The compressibility can be measured directly in a Coulomb blockade experiment, where it determines the spacing of peaks in the charge addition spectrum. As a function of doping away from half filling, one can distinguish three different regimes. At small doping the nonoverlapping soliton picture applies, making the compressibility (and hence the charging peak spacing) a function of density (Fig. 1). At somewhat higher doping, when the charge solitons overlap while the flavor fields at their cores do not, the peaks will be equally spaced, since the compressibility in this regime is density independent. The crossover density $n \simeq w^{-1}$ is sensitive to the magnetic field which controls soliton size $w = \hbar v/\Delta_{\text{ch}}$. Finally, at even higher doping, when the soliton cores overlap, the exchange effects set on, the neutral sector contribution to the energy becomes significant, and the peak spacing acquires period 4 in the electron number.

To summarize, the compressibility variation with soliton size is manifest in the charging spectrum near half-filling dependence on the magnetic field. Along with the power law field dependence (5) of the gap at half filling, it represents the novel 1D electron correlation phenomenon observable in a narrow gap state of nanotubes in thermodynamic equilibrium.

This work is supported by the MRSEC Program of the National Science Foundation under Grant No. DMR 98-08941 and by U.S. DOE under Contract No. DE-AC02-98CH10886.

[1] C. Kane, L. Balents, and M. P. A. Fisher, Phys. Rev. Lett. **79**, 5086 (1997).
[2] R. Egger and A. O. Gogolin, Phys. Rev. Lett. **79**, 5082 (1997).
[3] L. Balents and M. P. A. Fisher, Phys. Rev. B **55**, R11 973 (1997).
[4] Yu. A. Krotov, D.-H. Lee, and S. G. Louie, Phys. Rev. Lett. **78**, 4245 (1997).
[5] A. Odintsov and H. Yoshioka, Phys. Rev. Lett. **82**, 374 (1999).
[6] M. Bockrath *et al.*, Nature (London) **397**, 598 (1999).
[7] R. Egger *et al.*, cond-mat/0008008.
[8] A. Bachtold *et al.*, Phys. Rev. Lett. **87**, 166801 (2001).
[9] H. Ajiki and T. Ando, J. Phys. Soc. Jpn. **62**, 1255 (1993); **65**, 505 (1996).
[10] C. L. Kane and E. J. Mele, Phys. Rev. Lett. **78**, 1932 (1997).
[11] J.-O. Lee *et al.*, Solid State Commun. **115**, 467 (2000).
[12] C. Zhou *et al.*, Phys. Rev. Lett. **84**, 5604 (2000).
[13] S. J. Tans *et al.*, Nature (London) **386**, 474 (1997).
[14] M. Bockrath *et al.*, Science **275**, 1922 (1997).
[15] S. J. Tans *et al.*, Nature (London) **394**, 761 (1998).
[16] D. H. Cobden *et al.*, Phys. Rev. Lett. **81**, 681 (1998).
[17] J. Nygard *et al.*, Nature (London) **408**, 342 (2000).
[18] W. Liang *et al.*, Phys. Rev. Lett. **88**, 126801 (2002).
[19] R. Saito, G. Dresselhaus, and M. S. Dresselhaus, *Physical Properties of Carbon Nanotubes* (Imperial College Press, London, 1998).
[20] H. J. Shulz, cond-mat/9808167.
[21] H.-H. Lin, L. Balents, and M. P. A. Fisher, Phys. Rev. B **58**, 1794 (1998).
[22] A. B. Zamolodchikov and Al. B. Zamolodchikov, Ann. Phys. (N.Y.) **120**, 253 (1979).